Supporting Information for

Palladium Catalysts for Dehydrogenation of Ammonia Borane with Preferential B-H Activation

Sung-Kwan Kim,[†] Won-Sik Han,[†] Tae-Jin Kim,[†] Tae-Young Kim,[†] Suk Woo Nam,[‡] Mariusz Mitoraj,[§] Łukasz Piękoś, [§] Artur Michalak,[*,§] Son-Jong Hwang,[#] and Sang Ook Kang[*,†]

[†]*Department of Chemistry, Korea University, Chung-nam 339-700, Korea.* [‡]*Fuel Cell Center, Korea Institute of Science and Technology, Hawolgok-dong 39-1, Seongbuk-gu, Seoul 136-791, Korea.* [§]*Department of Theoretical Chemistry, Faculty of Chemistry, Jagiellonian University, R. Ingardena 3, 30-060 Kraków, Poland.* [#]*Division of Chemistry and Chemical Engineering, California Institute of Technology, Pasadena, CA 91125, USA.*

Contents

General Methods

Materials and Methods. All experiments were carried out under a nitrogen atmosphere using Schlenk techniques or in a HE-493 dry box (Vacuum Atmosphere Co. Hawthorne, CA, USA). The solvents were dried over Na (tetraglyme), Na/benzophenone (THF), and $CaCl_2$ (nitromethane) distilled under nitrogen, then deoxygenated prior to use. The deuterated solvents were dried through trap-to-trap distillation from Na (C_6D_6) and CaH_2 ($CDCl_3$) and deoxygenated using three freeze-pump-thaw cycles. A palladium sponge and nitrosonium tetrafluoroborate were purchased from Strem Chemicals (Newburyport, MA, USA). Catalysts **1**[1]and **3**[2] were prepared as previously described. $NaBH_4$, BH_3SMe_2, and all of the alkyl amines were used as received from their commercial sources. NH_3BH_3, $R^1{}_nNH_{3-n}BH_3$ (n = 1, R^1 = Me, Et, ^{i}Pr, Ph; n = 2, R^1 = Et) were prepared using previously reported methods.[3] NH_3BRH_2 (R = ^{i}Pr, Ph) was prepared from $LiBRH_3$[4] and $(NH_4)_2SO_4$ in THF with stirring at 40 °C over night. $NaBD_4$ was used as purchased from Sigma Aldrich (St. Louis, MO, USA). The partially- and fully-deuterated ammonia boranes (ABs) were prepared from deuterated starting materials as previously reported for NH_3BH_3.[5] Deuterated ammonium sulfate was prepared as previously reported.[6]

Synthesis of [Pd(allyl)(2,4-hexadiene)][BF_4] (2). The di-μ-dichloro-bis(η^3-allyl)dipalladium dimer (1.83 g, 5.0 mmol) and silver tetrafluoroborate (1.95 g, 10.0 mmol) in CH_2Cl_2 (50 mL) were stirred for 15 min. The 2,4-hexadiene (1.9 mL) was added and stirring continued for an additional 2 min. The mixture was filtered and the precipitate washed with 10 mL of CH_2Cl_2. Subsequently, Et_2O (150 mL) was added to the combined filtrate to produce a white precipitate which was filtered and dried. The obtained solid was dissolved in 70 mL of CH_2Cl_2, and that solution was repeatedly filtered through a tightly packed plug of cotton until the solution was clear. Et_2O (100 mL) was added to the combined mother liquid of CH_2Cl_2 to precipitate the product. After filtration, the product was dried *in vacuo* to produce an off-white solid. Yield: 2.3 g (73 %)**;** ^{1}H NMR (300.1 MHz, $CDCl_3$): δ 1.93 (d, 6H, C*H*$_3$), δ 2.60 (m, 2H, CH_3C*H*CH), δ 3.63 (d, 2H, C*H*), δ 3.90 (d, 2H, CHC*H*CH), δ 4.91 (d, 2H, C*H*), and δ 6.10 (m, 1H, C*H*).

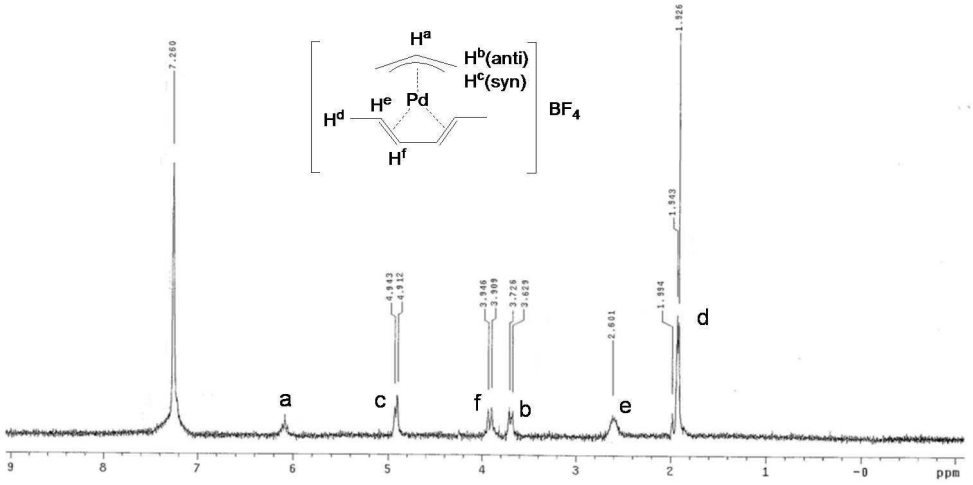

SFig-1. ^{1}H NMR spectrum of catalyst **2** along with its structure.

Analytical Methods. Solution NMR spectra were collected at room temperature using a Mercury-300BB spectrometer (Varian Inc., Palo Alto, CA, USA) unless otherwise stated. The spectral frequency was 96.3 MHz for ^{11}B and the NMR shifts in ppm were reported with reference to external standards of $BF_3{\cdot}Et_2O$ for the ^{11}B nucleus. ^{11}B solid state NMR experiments were performed using a DSX-500 spectrometer (Bruker AXS, Madison, WI, USA) and a boron-free, 4 mm CPMAS probe (Bruker AXS). Experimental details were described previously.[7] The spectral frequency was 160.5 MHz for ^{11}B and the NMR shifts in ppm were reported with reference to external standards of $BF_3{\cdot}Et_2O$ for the ^{11}B nucleus. Samples were loaded into a 4 mm ZrO_2 NMR rotor in Ar atmosphere inside a glove box. Dry nitrogen gas was used for sample spinning. The IR spectra were recorded on a Nicolet Avatar 330 FT-IR spectrometer (Thermo Fisher Scientific, Rochester, NY, USA) with a KBr pellet. Elemental analyses were performed using a Flash EA 1112 Series analyzer (ThermoQuest Italia SpA, Milan, Italy). Inductively coupled plasma-atomic emission spectroscopy was performed using a Varian 710-ES Model.

X-ray photoelectron spectroscopy (XPS) was carried out using the 8A1 beam line of the Pohang Light Source (PLS; Pohang Accelerator Laboratory, Pohang, Korea) and a laboratory-based ESCALAB 250 spectrometer (VG Scientific, Beverly, MA, USA) with a photon energy of 1486.6 eV (Al Kα).

Quadrupole mass spectroscopy (QMS) data were obtained using a SRS (Stanford Research Systems, Sunnyvale, CA, USA) RGA200 quadrupole mass spectrometer attached to a glass vacuum line system.

A Quattro Micro triple quadrupole mass spectrometer with an electrospray ionization source (Waters Corporation, Milford, MA, USA) was used in negative- and positive-ionization modes. The sample solution was directly infused at a flow rate of 100 μL/min using a syringe pump. The scanning mass range of the mass spectrometer was 5–2000 Da with a 0.5 Da step size. The capillary and cone voltages were set at 3200 V and 15–25 V, respectively, with nitrogen as the drying gas. The desolvation and cone gas flows were 350 L/h and 70 L/h, respectively. The desolvation temperature was 350 °C and the source temperature was 100 °C.

AB Dehydrogenation Procedure

Apparatus and procedure for Pd(II) catalyzed dehydrogenation. SFig-1 shows the experimental apparatus. The reactor consisted of modified 150 mL double jacket glassware. A three-way connector was modified to allow the system to be purged with argon gas and to allow the hydrogen gas produced during the dehydrogenation reaction to pass through the mass flow meter (MFM). The apparatus enabled the catalyst to be injected into the reactor without exposing the reactants to air. The reaction temperature was monitored and controlled with a thermocouple and an external heater/cooler (chiller), respectively. The experimental procedure involved filling the reactor with 2 mL of a tetraglyme solution containing 1.46 mmol of AB. The reactor was subsequently flushed with argon for at least 30 min to minimize the moisture level inside the vessel. After thermal equilibration of the reactor and the low temperature trap, 3 mol% of catalyst **3** was dissolved in 0.5 mL nitromethane ($MeNO_2$) and injected into the AB solution. Reaction time began at the time when the catalyst was introduced into the mixture and ended when H_2 evolution ceased. The progress of the reaction was monitored by examining the amount of hydrogen generated using a volumetric technique that allowed real time tracking of the reaction.[8] $MeNO_2$ (bp 101 °C) and other volatiles including NH_3 in the product stream were anticipated because of the large exothermy expected under the experimental conditions, even though the reactor temperature was controlled at 25 °C. In the apparatus, a −90 °C low temperature bath (liquid N_2 with CH_2Cl_2) trapped the volatiles to ensure that the gas volume measured as it passed through the MFM system was only due to hydrogen. After dehydrogenation, the solid remaining in the reactor was collected through filtration, rinsed with Et_2O and dried *in vacuo*. Because of the fast hydrogen release kinetics for catalyst **3**, there was the possibility of a heterogeneous pathway. That possibility was examined either by the supplemental addition of AB after dehydrogenation or through mercury poisoning[9] as previously described. The H_2 release

kinetics was not altered following either of those actions.

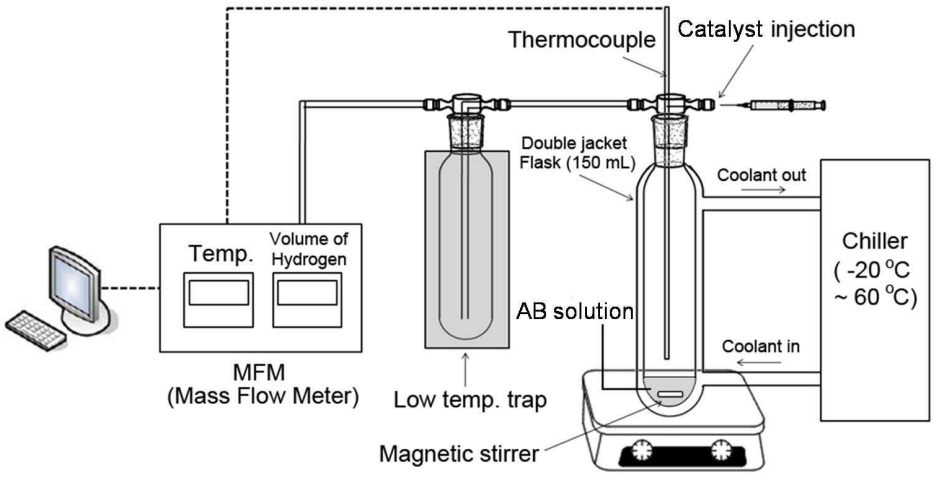

SFig-2A. Schematic diagram of the experimental apparatus used to determine H_2 release kinetics.

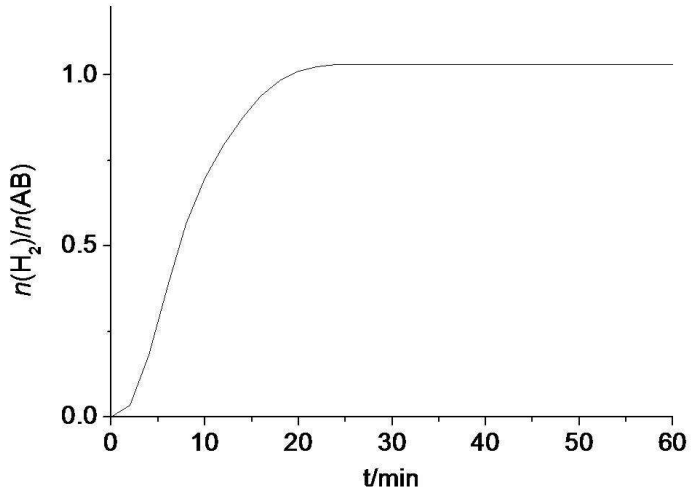

SFig-2B. H_2 release profile for solid AB at 100 ℃. That profile was used to calibrate the flow rate of the MFM portion of the apparatus.

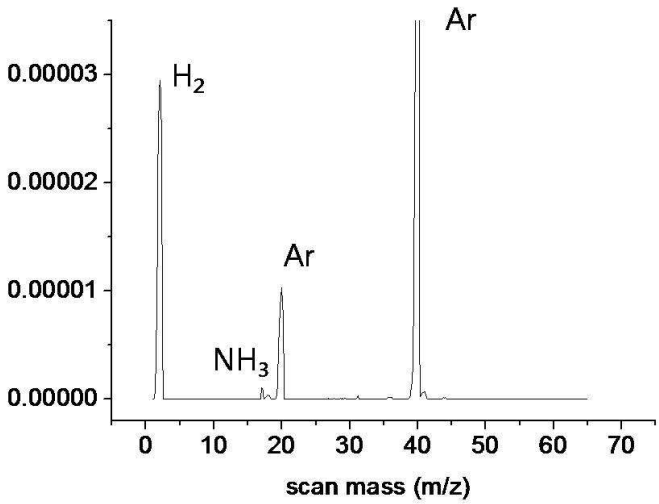

SFig-3. Mass spectrum of the volatile compounds from the AB dehydrogenation with catalyst **3** recorded at room temperature. Other than the intensity of the Ar carrier gas, the highest intensity mass number was *m/z* = 2.0 (H_2). A trace amount of *m/z* = 17.0 (NH_3) was detected.

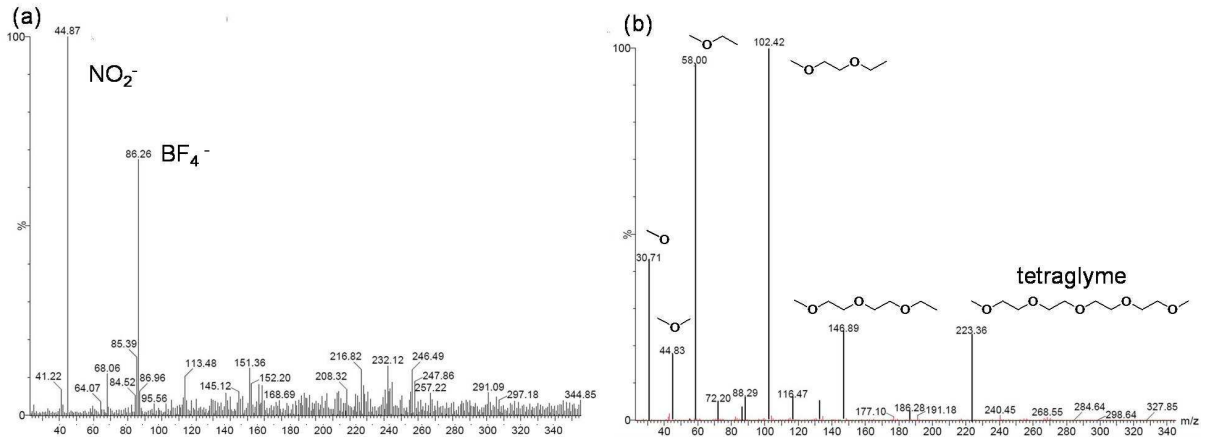

SFig-4. (**a**) Negative- and (**b**) positive-ion ESI mass spectra of a tetraglyme solution of the spent fuel acquired using a triple quadrupole mass analyzer. Following dehydrogenation, BF_4^- and NO_2^- were the only chemical substances identified in the tetraglyme solution.

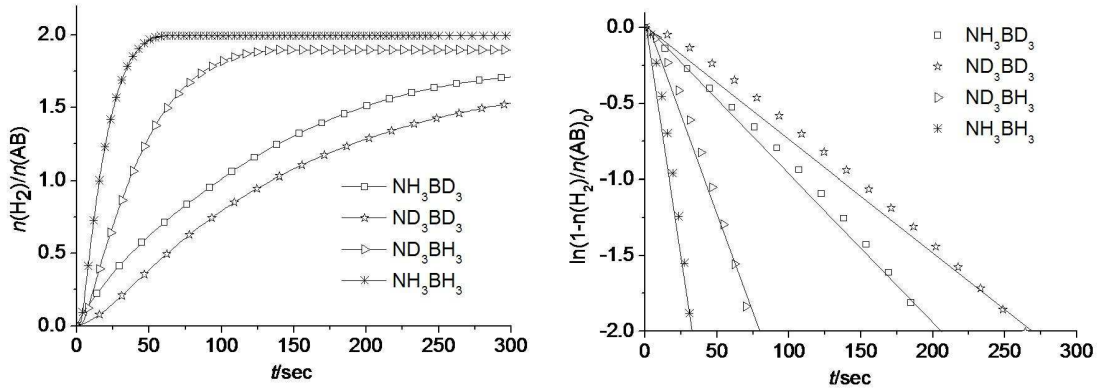

SFig-5. (**a**) Dehydrogenation kinetic isotope effect (KIE) plots for AB and deuterated ABs with catalyst **3** at 25 °C and (**b**) their corresponding logarithmic plots. The straight lines in (**b**) were obtained from linear regression analysis of the data points.

STable 1. Elemental analysis and formula of spent fuel

Method	Spent fuel components				
	B	N	H	Pd	Formula of spent fuel
EA[a]	-	0.95	4.50	-	$B_{1.00}N_{0.95}H_{4.50}Pd_{0.024}$
ICP[b]	1.00	-	-	0.024	
XPS[c]	1.00	0.7	-	-	$BN_{0.7}$

[a]Elemental analysis, [b]Inductively coupled plasma-atomic emission spectroscopy, [c]X-ray photoelectron spectroscopy

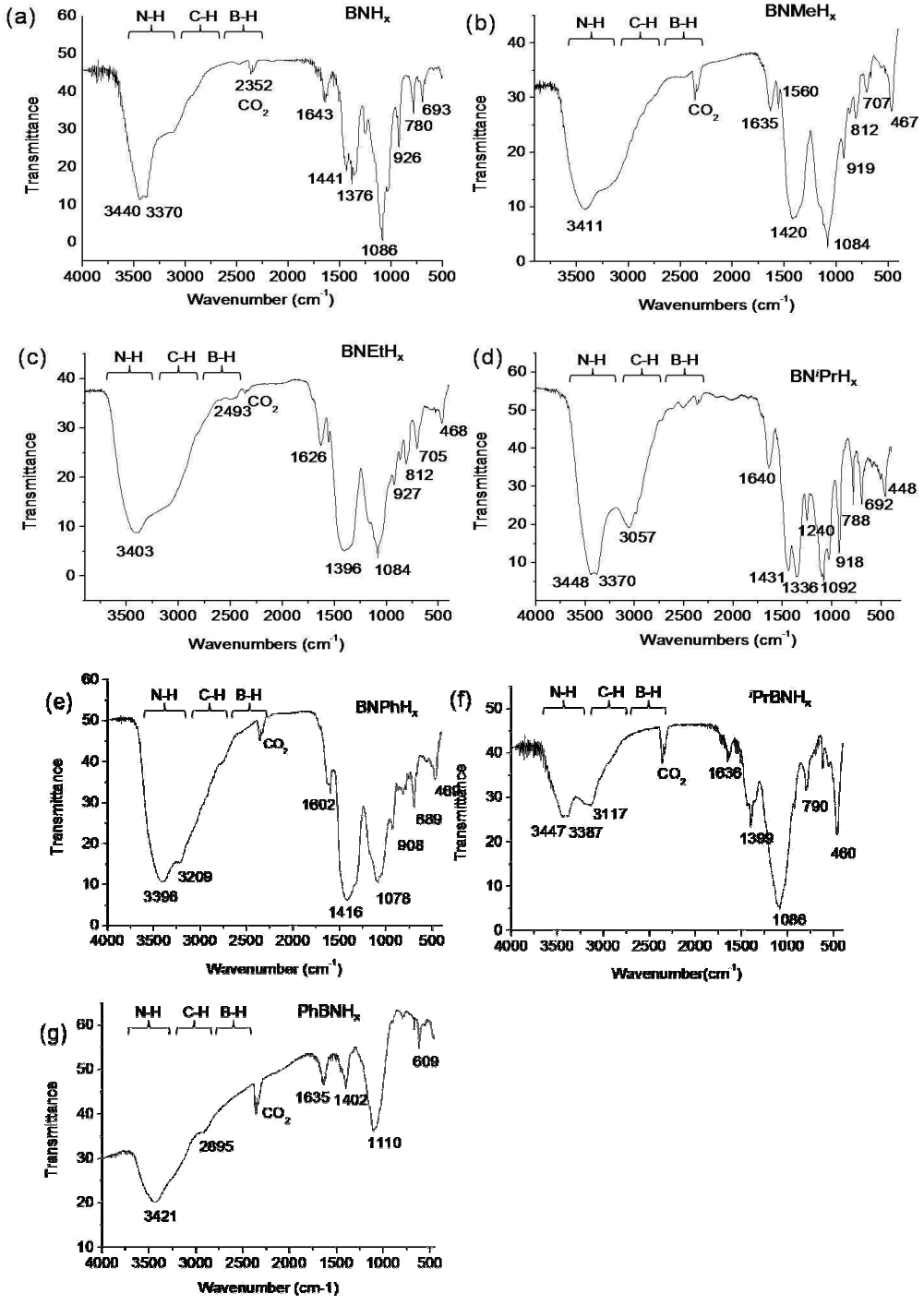

SFig-6. Infrared spectra of the spent fuels from a series of alkyl ABs: (a)BNH_x, (b) $BNMeH_x$, (c) $BNEtH_x$, (d) BN^iPrH_x, (e) $BNPhH_x$, (f) $^i PrBNH_x$ and (g) $PhBNH_x$.

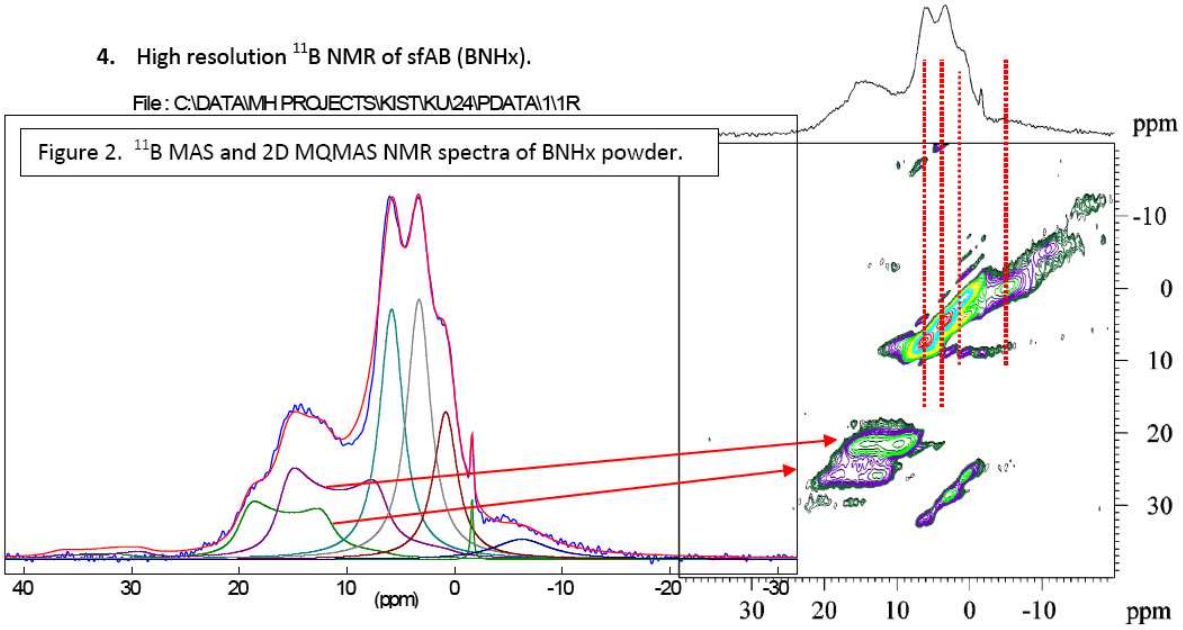

SFig-7. 1D ^{11}B MAS (left) and 2D ^{11}B MQMAS (right) NMR spectra of BNH_x powder.

First, a two dimension (2D) ^{11}B MQMAS NMR spectrum was obtained to sort out the non-equivalent boron sites that are indistinguishable in a one dimension (1D) MAS spectrum. Two groups of peaks were initially identified using this approach. The broad peaks between 10 and 20 ppm apparently originated from borons in a trigonal geometry (B^3) while the several sharp peaks in the +6~−6 ppm range were due to borons in a tetrahedral coordination. These tetrahedral borons (B^4) are believed to be responsible for the BN_4 or BHN_3 units in diamondoid type structures. Based on the 2D spectrum, the 1D spectrum was decomposed as in SFig-7 to 7 different sites. The respective peaks are compiled in STable 2. An additional resonance is seen at −10 ppm in the 2D spectrum, but it was ignored due to its negligible contribution. The 1D spectrum without ^{1}H decoupling allowed us to conclude that nearly all boron peaks except for the peaks at −6 ppm and −10 ppm are without direct B-H bonds. Moreover, nearly all peaks showed high efficiency in ^{1}H-^{11}B cross polarization MAS NMR, indicating that the borons are in close proximity to either NH or -CH_n organic species. Based on the spectral decomposition, the ratio of $[B]_{trigonal}$ to $[B]_{tetrahedral}$, or B^3:B^4, was calculated to be 2:3, a ratio that helped us to speculate on a possible structure. Lastly, the relatively sharp peak at -1.6 ppm is believed to be BF_4^-, although its bounding cation is not known.

STable 2. ^{11}B peaks from decomposition of 1D and 2D MAS NMR spectra

Chemical shift (δ_{iso})	C_Q^{10}	η^{10}	Intensity	Relative Intensity ratio	
21.6 18.4	2.53 2700	0.1 0.1	38.25 68.48	0.14 0.25	sp^2: 0.39
6.1 3.6 1.1	0.5 0.5 0.5	1 1 1	60.77 62.82 35.61	0.22 0.23 0.13	sp^3: 0.57
−6.0	0.5	1	11.80	0.04	BH_x
−1.6	-	-	-	<0.02	BF_4^-

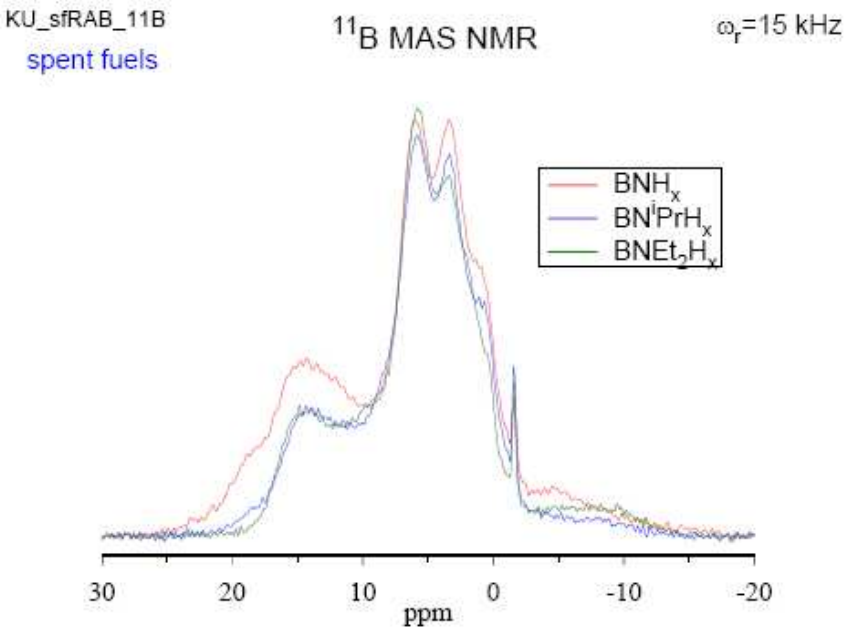

SFig-8. ^{11}B MAS NMR spectra of BNH_x, BN^iPrH_x and $BNEt_2H_x$.

Other spent fuels of sample entries 4 and 6 (Table 1): The boron sites found in BNH_x appeared similarly in both cases (see ^{11}B MAS NMR spectra in SFig-7) with an exception of the boron sites at 21.6 ppm (trigonal B^3).

Computational Details

DFT calculations based on the Becke-Perdew exchange-correlation functional[11-13] were performed using the Amsterdam Density Functional (ADF) program, version 2009.01.[14-18] Within the ADF program, a standard double-zeta STO basis with one set of polarization functions was applied for the H, C, and N atoms, while a standard triple-zeta basis set was employed for the Pd atom. The *1s* electrons of B, C, and N, as well as the *1s-3d* electrons of Pd were treated as a frozen core. Auxiliary *s, p, d, f,* and *g* STO functions, centered on all nuclei, were used to fit the electron density and obtain accurate Coulomb and exchange potentials in each SCF cycle. Relativistic effects were included at the level of ZORA approximation as implemented in the ADF program.[19] The natural orbitals for chemical valence (NOCV)[20-22] analysis, supported by the extended transition state (ETS) Ziegler-Rauk bond-energy decomposition scheme,[22,23] was performed for catalyst (**A**), to describe the bond between the AB molecule and the metal containing fragment. The combined ETS-NOCV approach[20] allowed us to separate the independent components of the differential density, $\Delta\rho$, into the electron charge transfer channels that contribute to the bonding between fragments in a molecule. That approach provides energetic estimates of the components' relative significance. In particular, in the case of transition metal complexes, the ETS-NOCV approach provides estimates of the independent contributions from ligand → metal donation and metal → ligand back-bonding.

Reference

1. Lai, T. W.; Sen, A. *Organometallics* **1984**, *3*, 366
2. Mathew, J. P.; Reinmuth, A.; Melia, J.; Swords, N.; Risse, W. *Macromolecules* **1996**, *29*, 2755.
3. Jaska, C. A.; Temple, K.; Lough, A. J.; Manners, I. *J. Am. Chem. Soc.* **2003**, *125*, 9424.
4. Singaram, B.; Cole, T. E.; Brown, H. C. *Organometallics* **1984**, *3*, 774.
5. Keaton, R. J.; Blacquiere, J. M.; Baker, R. T. *J. Am. Chem. Soc.* **2007**, *129*, 1844.
6. Käß, M., Friedrich A.; Drees, M.; Schneider, S. *Angew. Chem. Int. Ed.* **2009**, 48, 905.
7. Hwang, S.-J.; Bowman, R. C.; Reiter, J. W.; Rijssenbeek; Soloveichik, G. L.; Zhao, J.-C.; Kabbour, H.; Ahn, C. C. *J. Phys. Chem. C* **2008**, *112*, 3164.
8. Kim,S. J; Lee J.; Kong K. Y.; Jung, C. R.; Mina, I.-K.; Lee, S.-Y.; Kim H.-J; Nam S. W.; Lim T.-H. *Journal of Power Sources* **2007**, *170*, 412.
9. Jaska, C. A.; Manners, I. *J. Am. Chem. Soc.* **2004**, *126*, 9776.
10. Stowe, A. C.; Shaw, W. J.; Linehan, J. C.; Schmid, B.; Autrey, T. *Phys. Chem. Chem. Phys.* **2007**, *9*, 1831.
11. Becke, A. *Phys. Rev. A* **1988**, *38*, 3098.
12. Perdew, J. P. *Phys. Rev. B* **1986**, *33*, 8822.
13. Perdew, J. P. *Phys. Rev. B* **1986**, *34*, 7406.
14. te Velde, G.; Bickelhaupt, F. M.; Baerends, E. J.; Fonseca Guerra, C.; van Gisbergen, S. J. A.; Snijders, J. G.; Ziegler, T. *J. Comput. Chem.* **2001,** *22*, 931, and refs therein.
15. Baerends, E. J.; Ellis, D. E.; Ros, P. *Chem. Phys*. **1973**, *2*, 41.
16. Baerends, E. J.; Ros, P. *Chem. Phys*. **1973**, *2*, 52.
17. te Velde, G.; Baerends, E. J. *J. Comput. Phys*. **1992**, *99*, 84.
18. Fonseca Guerra, C. G.; Visser, O.; Snijders, J. G.; te Velde, G.; Baerends, E. J. In *Methods and Techniques in Computational Chemistry*, METECC-95; Clementi, E., Corongiu, G., Eds.; STEF; Cagliari, Italy, **1995**; p 303.
19. E. van Lenthe, E.; van Leeuwen, R.; Baerends, E.J.; Snijders, J.G. *International Journal of Quantum Chemistry* **1996**, *57*, 281.
20. Mitoraj, M.; Michalak, A; Ziegler, T. *J. Chem. Theory Comput.* **2009**, *5*, 962.
21. Mitoraj, M.; Michalak, A. *J. Mol. Model*. **2007**, *13,* 347.
22. Michalak, A.; Mitoraj, M.; Ziegler, T. *J. Phys. Chem. A*. **2008**, *112*, 1933.
23. Ziegler, T.; Rauk, A. *Inorg. Chem.* **1979,** *18*, 1755.